*Journal of Harbin Engineering University* Vol 44 No. 8
*ISSN: 1006-7043* August 2023

# Designing Of A Novel Approach For Image Haze Removal Using Color Attenuation Prior (CAP) And Single Scale Retinex (SSR) Hybrid Restoration & Enhancement Techniques

**Abhishek[1], Dr. Rajeev Ratan[2]**

Research Scholar,
Professor, Dept. of ECE, M.V.N. University, Palwal
Dept. of ECE, M.V.N. University, Palwal

**Abstract:**
*Haze is a poor-quality state described by the iridescent appearance of the atmosphere, which reduces visibility. It is caused by high concentrations of atmospheric air pollutants, such as dust, smoke, and other particles that scatter and absorb sunlight. Typically, the images captured in the outside environment have low contrast, color fade, and restricted visibility due to suspended particles of the atmosphere that directly influence the image quality. This can cause difficulty in identifying the objects in the captured hazy images or frames. To address this problem several image dehazing techniques have been developed in the past to address this problem, each of which has its advantages and limitations. Still, effective image restoration and enhancement remains a challenging task. Based on this reasoning, a novel hybrid mechanism is proposed in this research work by combining two existing methods: Color Attenuation Prior (CAP) and Single Scale Retinex (SSR).Regarding post-enhancement, SSR excels, whereas CAP is best served by image restoration and Haze removal. High image noise, poor contrast, a huge haze gradient, Halo Artefacts, lost detail, blurred images, edges that weren't preserved, etc., were all issues the hybrid approach resolved. Parameters including PSNR, SSIM, MSE, the Haze improvement index, and Visibility Metric (VM) have been calculated to evaluate the efficacy of the hybrid approach. The proposed approaches are implemented using the generalized and image processing toolboxes in MATLAB 2016a. Experimental results show that the proposed approach outperforms state–of–the–art haze removal algorithms.*

**Keywords:** *Color Attenuation Prior, Single Scale Retinex Depth Map, Histogram Equalization, Peak Signal to Noise Ratio, Mean Square Error, Structure Similarity Index Measure, Visibility Metric.*

## 1. INTRODUCTION

Images of outdoor scenes are usually degraded by the turbid medium (e.g., particles, water droplets) in the atmosphere. These phenomena, which are caused by air absorption and scattering, include haze, fog, and smoke. Along the line of sight, the camera's exposure to the scene point's irradiance is reduced. Furthermore, the incoming light is blended with the airlight (ambient light reflected into the line of sight by atmospheric particles). The degraded images lose the contrast and color fidelity [1]. Haze removal (or dehazing) is highly desired in consumer/computational photography and computer vision applications. First, removing haze can significantly increase the scene's visibility and correct the color shift caused by the air light. In general, the haze-free image is more visually pleasurable. Second, most computer vision algorithms, from low-level image analysis to high-level object recognition, usually assume that the input image (after radiometric calibration) is the scene radiance. The performance of vision algorithms (e.g., feature detection, filtering, and photometric analysis) will inevitably suffer from the biased, low-contrast scene radiance. Last, haze removal can produce depth information and benefit many vision algorithms and advanced image editing. Haze or fog can be a helpful

depth clue for scene understanding. The haze removal techniques can be classified into two categories: image enhancement and image restoration. Image enhancement doesn't include the reason why fog degrades image quality. This technique enhances the contrast of haze image but leads to loss of information.[2] Image restoration studies the physical procedure of imaging in fog**.** Two main types of image dehazing techniques exist: single-image dehazing and multiple-image dehazing. Techniques based on wavelets, Retinex theory, homomorphic filtering, and histogram equalization are only a few examples of enhancement-based methods[2]. After decades of development, the SSR has evolved into the multiscale weighted average Retinex algorithm (MSR), the Retinex algorithm's improved version (MSRCR), and various variants. Combining alternative algorithms with classical ones Retinex theory is essential to image enhancement technologies [3] because of its consistent color reasoning.

This paper is structured as follows. In Section II, we will talk about the literature review of the CAP and SSR methods. Advanced image restoration and enhancement methods are explained in Section III, along with their hybrid approach. In Section IV, we conduct a series of randomized experiments to assess the efficacy of the proposed hybrid algorithm and compare it to more traditional approaches. Section V provides a brief conclusion and an overview of the proposed research's potential future directions.

## 2. LITERATURE REVIEW

Zhu et al.(2014) introduced a straightforward yet effective prior for eliminating fog from a solitary foggy input image . A sequential model depicting the scene profundity of the foggy image under this groundbreaking prior might be established to restore the profundity data proficiently, and its variables can be educated through directed learning. By alluding to the blurry image's profundity map, authors can swiftly and effortlessly eradicate all indications of mist from a solitary image [1].

Balakrishnan and James (2017) proposed an innovative linear chromatic reduction prior grounded on the luminosity and intensity of pixels in the foggy image. The authors formulated a sequential blueprint for the scene profundity of the blurry image employing this uncomplicated yet effective prior, and subsequently employed supervised education to establish the blueprint's parameters. Consequently, the authors stated that a blurry image's scenery brightness could be rapidly restored. Scene distance is computed using uncomplicated linear model formulas, and the essential variables are obtained from the linear model to streamline scene restoration. [2].

Yu et al. (2018) established the ACM SIG Proceedings formatting guidelines and presented the chromatic reduction prior fog elimination technique. The authors additionally offered a groundbreaking resolution in certain instances. The authors additionally introduced a hierarchical exploration technique for predicting atmospheric brightness based on a quad-tree partition to enhance the algorithm's accuracy. [3].

Thepade et al. (2018) additionally introduced a hierarchical exploration technique for predicting atmospheric brightness based on a quad-tree partition to enhance the algorithm's accuracy. The authors additionally offered a fusion-oriented method that offers exceptional mist elimination in contrast to the traditional mist elimination approaches. [4].

A sequential profundity framework founded on hue weakening was proposed by Raikwar and Tapaswia (2019) prior to ascertaining landscape profundity from a solitary image. It is founded on the revelation that the disparity between saturation, luminosity, and tint escalates with scene profundity and preserves the structural similarity of the deteriorated image. Moreover, it could mend the limits of the setting without disrupting the current ones. [5].

Huang et al. (2019) proposed a variogram- and hue-based remote sensing image dehazing technique. It was revealed that subjective visual impact and objective assessment indicators significantly prefer the restored images generated by this technology over the original fuzzy images. UAV distant sensing images captured in mist can be substantially enhanced due to the immense enhancement in the images' clarity, mean slope, and data entropy. [6].

With their proposed solitary-image mist elimination method, Ngo et al. (2019) exhibit a remarkable enhancement over the chromatic reduction prior-dependent approach. Given that the color weakening prior's antecedents do not consistently uphold, concerns such as hue alteration and ambient interference have arisen. The recommended approach by the authors surpasses previous cutting-edge algorithms on simulated and real datasets of foggy images concerning both numerical assessments and subjective visual excellence. [7]. Wang et al. (2019) proposed a solitary novel image dehazing technique for foggy images, encompassing artificial and actual-

world. Based on the revelation that pixel values in a foggy image can be characterized as lines in the RGB color spectrum that intersect at the atmospheric brightness, the authors propose a dehazing method that amplifies color weakening in two manners. the authors initially employed the misty streaks before approximating aerial illumination. The perpetual dispersal coefficient should be substituted second. [8]. Kansal and Kasana (2020) proposed a CAP-dependent de-fogging method. CAP compared the profundity of a misty, murky impact at every pixel because of the discrepancy between its intensity and luminosity. The minimal manipulation is executed on a nearby pane to reduce the depth map estimated duration. The profundity map's minuscule border characteristics are restored using a gradient realm-directed image filter. The authors presented an innovative method for post-editing the de-misted image to eradicate the challenge caused by errors in approximating worldwide ambient illumination. It rapidly achieved object-free, concurrent dynamic scope alteration, hue consistency, and illumination depiction. [9]. HRNSCT was formulated by Zhang et al. (2021) to clarify foggy images. HRNSCT reduces both low- and high-frequency mist. A misty, disorderly hue image is divided into low- and high-frequency orientations by NSCT. The authors stated that the transmission chart lessens disturbance and enhances dehazed image particulars by reducing and amplifying the three channels' high-frequency orientation sub-bands.[10]. Tang et al. (2022) introduced a hue reduction prior defogging method and an optimization strategy based on hue reduction prior to tackle the problem of image smudging in high-frequency regions of close-up sight. The non-linear scene profundity blueprint is re-established by augmenting the scene profundity approximation data to recognise the precise scene profundity depth. The authors employed a binary tree exploration method to discover the ideal surrounding illumination value, and in the end, a collection of variables is modified to enhance the model. [11]

In 2017, Tang et al. proposed an enhanced Retinex image improving technique based on the guided filter in the IHS color area. The authors utilised a directed filter to enhance high-frequency data in order to obtain intricate-scale precision. And subsequently regained low-frequency data by employing a directed filter to break down information in the logarithmic realm; conversely, the retinex method solely extracts high-frequency data to enhance the image. The authors merged the image's elevated- and diminished-pitch data to generate a composite image. [12]. Faraj and Abood (2017) unearthed superior differentiation, boundaries, and image attributes using solitary-scale retinex. Various magnitude retinex enhanced the image sharpness and excellence. MSR improved the images' brightness and characteristics. This technique demonstrated its efficacy in all thermal visuals and greatly enhanced them. [13]. The twofold connection between image dehazing and nonuniform brightness division was mathematically exhibited by Galdran et al. (2018), who demonstrated that implementing a Retinex procedure to a reversed image and subsequently changing the outcome clears the haze of the image and vice versa. The authors have demonstrated, theoretically and empirically, that this applies to numerous Retinex techniques. Both numerical and descriptive testing revealed competitive dehazing outcomes [14]. Li et al. (2018) proposed merging Retinex and a dim channel to dehaze sea cucumber images. The dim channel is utilised to pre-process the authentic RGB image, and a pondered mean of the pixels is employed to uphold the mirroring quality of the image. To enhance the depiction, it is convolved with a Gaussian blueprint. The luminosity and intensity of an HSV image are enhanced by adjusting the S and V variables. [15]. Two prototypes, blurry occurrence illumination and misty mirrored illumination, were proposed by Liu et al. in 2020. The dim passage clearing technique has reevaluated the surrounding luminosity value, the transparency of the mist incoming light element, and the mist mirrored light element. Consequently, Retinex's haze-resistant image exhibits more significant disparity and luminosity [16].

Guo & Wang (2020) proposed an amalgamated booster. The shadow passage prior and retinex models are linked using two adaptable parameters to generate DeRetinex. The subsequent improvement employs the DeRetinex framework, eradicating the mist formed by dehazing. The recommended method prevents excessive exposure and offers abundant texture characteristics, minimal interference, and outstanding color restoration [17]. To foresee the brightness diagram, HUANG et al. (2020) presented a comprehensive network structure relying on Retinex. IEB integrates a focus technique to reduce image imperfections and soften hue shifts. The authors merged the image with the nearby grey cover to generate nonuniform brightness image combinations to encourage data variety and model generalization [18]. The CNR which clarifies the original foggy

images, was proposed by Sai Kumar et al. (2020) as a technique for assessing foggy and misty images. The authors also proposed a unique, original effective parameter based on an image-filtering method[19]. Employing the Ivory-Patch Retinex algorithm and an enhanced dim channel prior approach, Chung et al. (2020) proposed a technique for eliminating fog from a solitary image (both diverse algorithms). The algorithm's worth increases as the structure becomes increasingly varied. With its groundbreaking design and superb execution, the proposed algorithm can restore a pristine image while tackling the aura effect, chromatic aberration, and protracted operation durations[20]. A Bayesian retinex method was formulated by Zhuang et al. in 2021 to amplify underwater images with multi-level reflectance and illumination gradient priors. Basic hue adjustment is employed to eliminate color tints and revive authenticity. Next, employ multi-order gradient priors on hue and lighting to enhance the color-adjusted image. [21].
Khalil and Ameen (2022) formulated the SSR method to enhance nocturnal image manipulation. Initially, it transformed the RGB image to HSV and improved the V channel while keeping the H and S channels unaltered. Then it calculated the enlightened and authentic images' logarithms and deducted them using an alternative approach [22].

## 3. PROPOSED METHODOLOGY

Combining Color Attenuation Prior (CAP) with Single Scale Retinex (SSR) to eliminate haze in images is the focus of the proposed hybrid approach. Here is a rundown of what goes down with the hybrid approach:

### 3.1. Color Attenuation Prior (CAP):

It's a novel linear approach that considers how different pixels in hazy images vary regarding brightness and saturation. Recovering a dehazed image from an input image requires color attenuation to first detect or estimate at certain features associated with the original image[15,16]. Four stages are numbered one through four to color attenuation-based haze reduction methods.

#### i. Atmospheric Scattering Model

McCartney proposed a model of air scattering to explain the fuzzy image [20]. Here, list the equation used in the model of atmospheric scattering.

$$I(x) = J(x)t(x) + A(1 - t(x)) \quad (1)$$

$$t(x) = e^{-\beta d(x)} \quad (2)$$

Here, I=hazy image, J=scene radiance, A=atmospheric light, β=scattering coefficient, x=pixel location, t=transmission medium, and I, J, and A represent three-dimensional vectors in RGB. T may be calculated using the second equation if the depth is known. The brightness is modest and the saturation is strong in typical, haze-free images. However, the opposite is true for fuzzy images. Due to the low saturation and strong brightness, images captured in fog might seem white. Since the haze's concentration increases with increasing scene depth, we may conclude that the two are positively related. According to many studies, the amount of haze is established by the disparity between brightness and saturation. [21].

Equation 1 is the one in which the whole color attenuation process works.

$$d(x) \alpha c(x) \alpha v(x) - s(x) \quad (3)$$

In this formula, the letters d, c, v, and s represent depth, haze density, luminance, and saturation. Here, factors like depth, haze concentration, and brightness and saturation differences all rely linearly on one another, making this model linear.

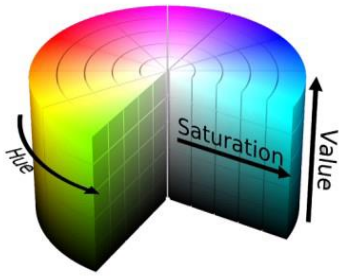


Fig 1: The HSV color model

$$d(x) = \theta_0 + \theta_1 v(x) + \theta_2 s(x) + \varepsilon(x) \quad (4)$$

Where $x$ is the position within the image, $d$ is the scene depth, $v$ is the brightness component of the hazy image, $s$ is the saturation component, $\theta_0$, $\theta_1$, $\theta_2$ are the unknown linear coefficients, $\varepsilon(x)$ is a random variable representing the unexpected error of the model, ε can be regarded as a random image. Here, d, v, s represent depth, brightness, and saturation. One of the most essential advantages of this model is that it has an edge-preserving property. To illustrate this, we calculate the gradient of $d$ in Equation (4), and

we have to prove the above equation gradient of d is calculated.

$$\nabla d = \theta_1 \nabla_v + \theta_2 \nabla_s + \nabla_\varepsilon \qquad (5)$$

Given that luminosity and intensity are two monochromatic images into which I, precisely the foggy image, is divided, equation (5) verifies that d possesses solely one boundary in I, thereby allowing us to assert that "This linear model accentuates the edge-conserving characteristic through which the depth data can be effectively restored even near the depth inconsistencies within the scene."

**ii. Estimation of the linear coefficient matrix:**

The linear coefficients (0, 1, and 2) in equation (4) are estimated with the help of supervised learning. The ground truth map and blurry image are included in the training data. Coefficient values may be applied to any fuzzy image once they are calculated. Their parameters [15,16] will be utilised to reconstruct the scene depth of the blurry original.

**iii. Estimation of depth information**

According to Zhu's research [3], the saturation and brightness of a pixel in a foggy region drastically change with the concentration of fog in a foggy image. In non-hazy locations, pixels have about the same brightness and saturation. When fog is present, the fog-free area's pixels gradually brighten. The saturation of the pixels begins to decline dramatically, creating a greater contrast between the brightness and the saturation of the pixels. This demonstrates a correlation between fog density and pixel brightness and saturation (VSD). The link between fog concentration and VSD is translated into the relationship between scene depth and VSD [3];
a depth map may be generated using the linear equation (4) since fog concentration is difficult to determine or estimate. Reconstructing transmission maps is another possible use of this method. This simplifies the process of dehazing both depth maps and gearbox maps. However, there are situations in which this strategy may not work. White objects, for example, tend to have high brightness and low saturation. Consequently, the proposed model is biased towards considering white objects in the image to be in the background. Unfortunately, this misinterpretation might cause an inaccurate depth measurement in some situations.

For this problem, we need to consider every possible pixel. We apply the following steps to the raw depth map, under the assumption that the scene's local depth is constant:

$$dr(x) = \min_{y \in \Omega_r(x)} d(y) \qquad (6)$$

Where $\Omega_r(x)$ is an $rxr$ neighborhood centered at $x$, and $dr$ is the depth map with scale $r$. However, it is also evident that the blocking artifacts appear in the image. To refine depth map, we use guided image filtering to smooth the image.

**iv. Estimation of atmospheric light & Scene Radiance Recovery**

Although the input blurry image's depth map was retrieved, the scene's depth distribution was already known. Darker areas of the map show locations further away. However, suppose we know the scene depth d and the ambient light. In that case, we can readily estimate the transmission t and recover J. Transmission t(x) may be roughly calculated given the depth and ambient light. The scattering coefficient is employed in both equations (1) and (2), hence it indirectly influences the dehazing intensity. The transmission t(x) is constrained to fall between 0.1 and 0.9 to limit background noise. Select the pixel with the greatest intensity in the matching blurry images, found within the top 0.1 percent brightest in the depth map. Atmospheric light causes me to be among these brightest pixels, and J scene radiance can be recovered as per equation 1.

**3.2 Single Scale Retinex (SSR):**

According to retinex theory, image I comprises lighting information L, which establishes the image's dynamic range, and reflection information R, which is the object's reflection information. Let $I(x, y)$ represent a pixel in the image $I$, $I(x, y)$ can be denoted by

$$I(x, y) = L(x, y).R(x, y) \qquad (7)$$

Retinex-based image enhancement involves keeping the reflection information while removing or reducing the effect of light information from the original image. Eq. (7) may be written as follows:

$$R(x, y) = I(x,y) / L(x, y) \qquad (8)$$

For the convenience of calculation, logarithmic transformation is implemented on both sides of Eq. (8) to estimate $R(x, y)$:

$$\log R(x, y) = \log I(x, y) - \log L(x, y) \qquad (9)$$

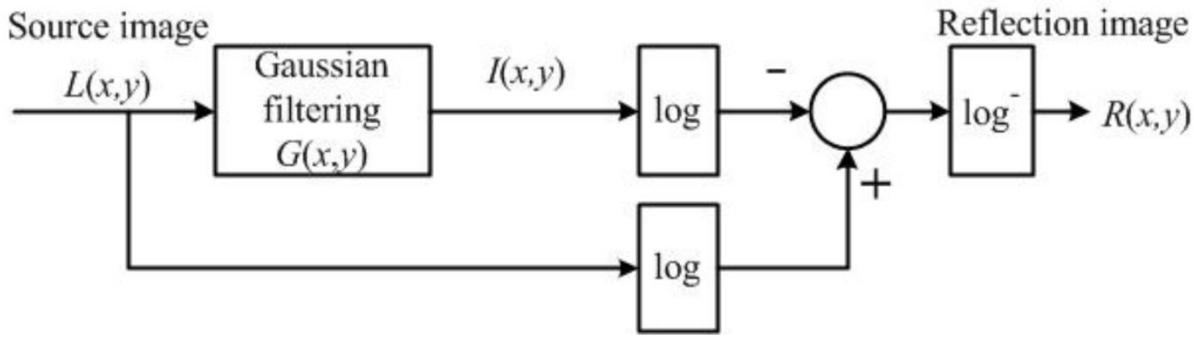


Fig 2. Basic flowchart of Retinex

$L(x, y)$ can be estimated by convolving $I(x, y)$ with a Gaussian function $G_\sigma(x, y)$

$$L(x, y) = I(x, y) * G_\sigma(x, y) \quad (10)$$

Where σ is the standard deviation of the Gaussian function, "*" denotes convolution operation,
$G_\sigma(x, y)$ is given by

$$G_\sigma(x, y) = \frac{1}{\sqrt{2\pi\sigma}} \exp(-{x^2 + y^2}/{2\sigma 2}) \quad (11)$$

Put Eq. (10) and Eq. (11) to Eq. (9), SSR is obtained as:

$$logR(x, y) = logI(x, y) - log[I(x, y) * G(x, y)] \quad (12)$$

Then, the reflection information $R(x, y)$ is computed by linear stretching log $R(x, y)$ instead of implementing exponent arithmetic:

$$R(x, y) = 255 \cdot \frac{\log R(x,y) - \min(logR(x,y))}{\max(logR(x,y)) - \min(logR(x,y))} \quad (13)$$

Where *min* ($log\ R(x, y)$) indicates the least of $log\ R(x, y)$, *max* ($log\ R(x, y)$) means the highest possible of $log\ R(x, y)$

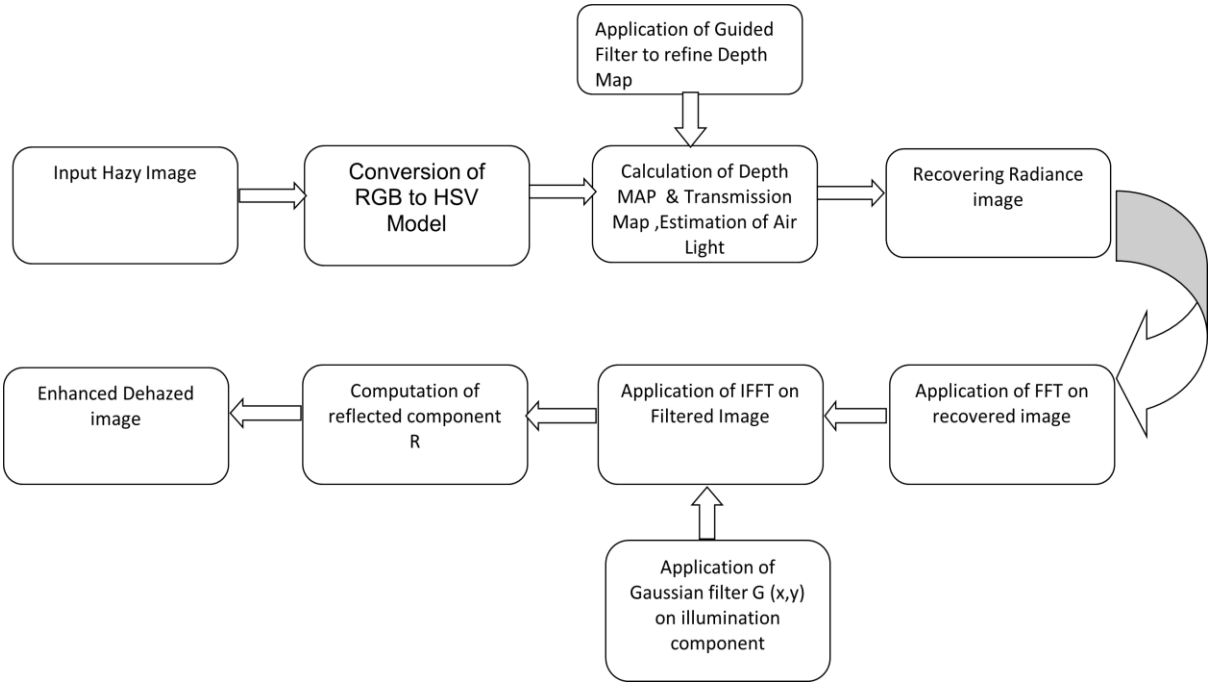


Fig3.Block Diagram of Proposed Methodology Hybrid CAP with SSR

Listed below are some implementation steps

1. Insertion of a Hazed Image
2. Conversion from RGB to HSV Model
3. Calculation of Depth Map & Transmission Map
4. Estimation of Air light
5. Application of Guided Filter to Refine Depth Map
6. Recovery of Radiance Image
7. Application of FFT on recovered Images through CAP
8. Application of Gaussian Filter on illumination component of the recovered image
9. Application of IFFT on Filtered image
10. Computation of the Reflected component of the image
11. Application of adaptive Histogram Equalization on Reflected Components
12. Obtaining the recovered enhanced Haze free image

**Embedding Tests:**

As discussed above, performance assessment parameters, i.e., PSNR, MSE, SSIM, and VM, have been taken to assess the operational effectiveness of the proposed hybrid CAP with the SSR method with the existing DCP method.

- PSNR: To evaluate the quality of the reference and dahazed images, the PSNR is used. The MSE between the pixel estimations of the referenced image (I) and the dehazed image (Iw)serves as a measure of PSNR

$$\mathrm{PSNR} = 10\log\frac{\max(I,Iw)^2}{\mathrm{MSE}} \qquad (14)$$

Where $\max(I, Iw)$ is the highest valued pixel of the image, in a grayscale image, this value is equivalent to 255. Better results are achieved with higher PSNR values.

- MSE: A well-known quality metric is needed to anticipate the inaccuracy between the referenced image (I) and the restored dehazed image(Iw). It is the mean squared difference between the original and degraded images. MSE's value ranges from 0 to ∞. Consequently, to reduce inaccuracy, it should be close to 0. The following mathematical formula can be used to calculate MSE:

$$\mathrm{MSE}\frac{1}{\mathrm{MN}}\sum_{i=1}^{M}\sum_{j=1}^{N}(I(i,j)-Iw(i,j))^2 \qquad (15)$$

I(i, j) and Iw(i, j) represent the pixel intensities of a haze-free referenced image and restored dehazed images; i and j represent the pixel coordinates. The parameters M and N specify the number of columns and rows. The highest possible value of R for an RGB image is 255.

- SSIM: Structure Similarity Index Measure is a perception-based model that considers key perceptual phenomena like brightness and contrast masking terms and views image deterioration as a perceivably altered structural aspect of the information.

$$\mathrm{SSIM}\ (I,Iw) = \frac{(2\mu x\mu y + C1)\ (2\sigma xy + C2)}{(\mu x2 + \mu y2 + C1)\ (\sigma x2 + \sigma y2 + C2)} \qquad (16)$$

$\mu_x$, $\mu_y$, $\sigma_y$ represent the corresponding average and variance values between the original referenced image I and the restored dehazed image $I_w$
$\sigma_{xy}$ represents the covariance between I & $I_w$
$C_1$& $C_2$ are constant factors.

## 4. EXPERIMENTAL RESULTS & DISCUSSIONS

This research work proposes a novel hybrid mechanism through the combination of CAP and SSR techniques. Firstly, the test image is restored using CAP method, followed by SSR to enhance the restored image and for the post-processing. The hybrid method is improved using the combination of Gaussian and guided filters to remove Halo artifacts and preserve edges, enhancing contrast and blurriness. Standard performance evaluation parameters, including PSNR, SSIM, MSE, and VM, have been computed and are being used to assess the effectiveness of the hybrid technique.

To showcase the outcome of each significant

step, an example of a test hazy image, "road.jpg" has been demonstrated in Fig. 4. Apart from it, four test hazy images 'forest.jpg','tree.jpg','mountain.png' and 'hoarding.png' has been dehazed through the proposed method and compared with existing method DCP and our earlier method DCPSSR. The comparison is demonstrated in Fig. 5. Here, the differences between the output images from the current DCP, our previous research DCPSSR, and the proposed hybrid technique is noticed.

By analyzing Fig. 5 it is quite visible that the proposed hybrid methodology outperforms the current DCP method and our previous research regarding image quality, dehazing and contrast.


(a)

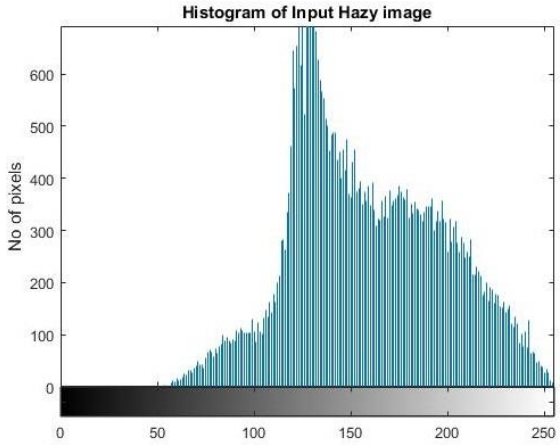


(b)

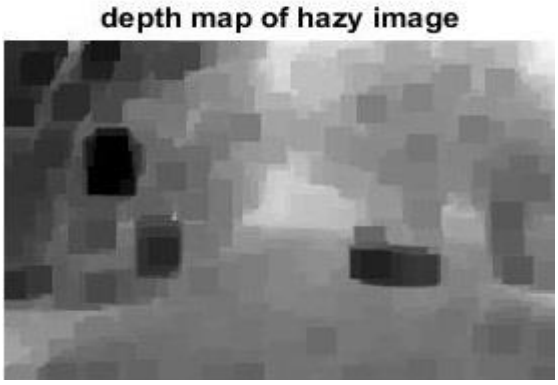


(c)

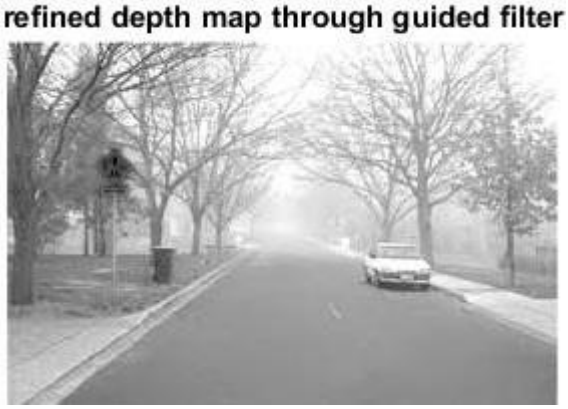


(d)


(e)

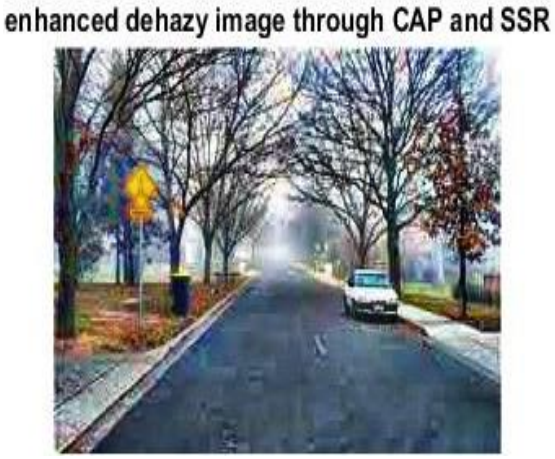


(f)

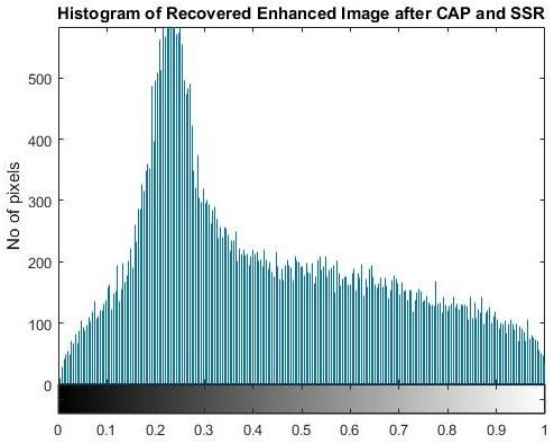


(g)

Fig4. (a)Hazy Input image (b) histogram of input Hazy image (c) depth map of input hazy image (d) refined depth map through guided filter (e) radiance dehazed image through CAP method (f) Recovered enhanced image through proposed CAP SSR (g) Histogram of Recovered Enhanced image after CAPSSR

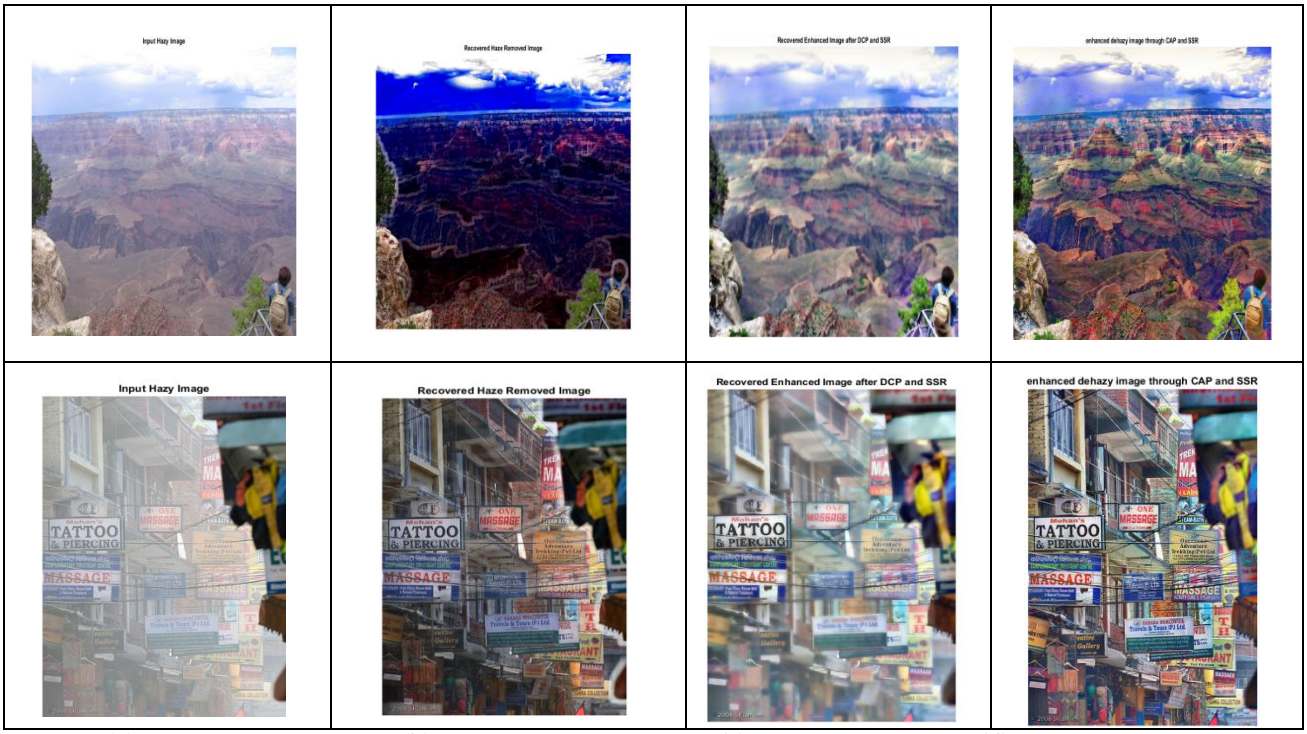


Figure 5: (a) (Far Left ) Hazed Input Images, (b)(Right to Left) DCP Output Images, (c)(Third to Fourth) DCPSSR Output Images, (d)(Far Right) Proposed Method Output Images.

After visually analyzing the proposed method efficiency, it is time to analyze it through standard performance assessment parameters. The experiment uses four hazy images: forest.jpg, tree.jpg, mountain.png and hoarding.png. The four performance evaluation metrics (MSE, PSNR, SSIM, and VM) that were previously discussed are used to compare values in Tables 1 and 2.

Table 1: Experiment Results Using a Guided Filter and the Prevalent DCP technique

| Image Name | PSNR | MSE | SSIM | VM |
|---|---|---|---|---|
| Forest.jpg | 67.77 | 0.0109 | 0.8503 | 32.02 |
| Tree.jpg | 64.79 | 0.0216 | 0.6746 | 54.05 |
| Mountain.png | 60.96 | 0.0405 | 0.5725 | 35.25 |
| Hoarding.png | 63.23 | 0.0309 | 0.6613 | 94.31 |

Parameter values for the DCP technique using a guided filter for all four images are shown in table 1.

Table 2 compares the outcomes of our experiments with those of our previous studies Hybrid DCP and SSR technique

| **Image Name** | **PSNR** | **MSE** | **SSIM** | **VM** |
|---|---|---|---|---|
| Forest.jpg | 70.74 | 0.0055 | 0.6261 | 108.68 |
| Tree.jpg | 66.68 | 0.0140 | 0.552 | 53.66 |
| Mountain.png | 71.45 | 0.0047 | 0.7273 | 38.15 |
| Hoarding.png | 69.67 | 0.007 | 0.6359 | 98.86 |

Table 3 Experimental Results with Proposed hybrid CAP and SSR technique

| Image Name | PSNR | MSE | SSIM | VM |
|---|---|---|---|---|
| Forest.jpg | 68.24 | 0.0098 | 0.5488 | 121.97 |
| Tree.jpg | 69.37 | 0.0075 | 0.695 | 97.09 |
| Mountain.png | 68.36 | 0.0095 | 0.6148 | 100.44 |
| Hoarding.png | 67.58 | 0.0114 | 0.6766 | 134.89 |

The parameter values for all four Images are shown in Table 3, illustrating the proposed method's validity.

Table 4 shows the similarities and differences between our proposed technique, the DCP method, and our previous research, DCPSSR.

Table 4: Comparison of Current and Proposed Approaches

| IMAGE NAME | PSNR | | | MSE | | | SSIM | | | VM | | |
|---|---|---|---|---|---|---|---|---|---|---|---|---|
| | DCP | DCP SSR | Proposed Method | DCP | DCP SSR | Proposed Method | DCP | DCP SSR | Proposed Method | DCP | DCP SSR | Proposed Method |
| Forest.jpg | 67.77 | 70.74 | 68.24 | 0.0109 | 0.0055 | 0.0098 | 0.8503 | 0.6261 | 0.5488 | 32.02 | 108.68 | **121.97** |
| Tree.jpg | 64.79 | 66.68 | **69.37** | 0.0216 | 0.0140 | **0.0075** | 0.6746 | 0.552 | **0.695** | 54.05 | 53.66 | **97.09** |
| Mountain.png | 60.96 | 71.45 | 68.36 | 0.0405 | 0.0047 | 0.0095 | 0.5725 | 0.7273 | 0.6148 | 35.25 | 38.15 | **100.44** |
| Hoarding.png | 63.23 | 69.67 | 67.58 | 0.0309 | 0.007 | 0.0114 | 0.6613 | 0.6359 | 0.6766 | 94.31 | 98.86 | **134.89** |

Table 4 shows that the proposed hybrid strategy significantly increases visibility because the VM quality index values are substantially greater than the DCP techniques already in use and our previous research DCPSSR. Analyzing all four images and their output and comparing them to the present DCP and the previous research, the hybrid approach that has been proposed enhances PSNR to 69.37 dB, whereas its ranges 67.77 dB in case of DCP and 71.45 dB DCPSSR, respectively. Similarly, the maximum VM value of the proposed hybrid technique is 134.89, whereas its only 94.31 and 108.68 in case of DCP and DCPSSR. The results are quite different if we look at the case of MSE and SSIM. For the proposed method, the minimum MSE value among all four images lowers to 0.0075, whereas its 0.0109 for DCP and only 0.0047 for DCPSSR. In the same way, for the proposed method, the maximum SSIM is 0.695, whereas its 0.8503 for the DCP and 0.7273 for DCPSSR.

Table 4 displays the calculated values of Performance assessment parameters demonstrate that the proposed hybrid technique excels above the DCP method and our previous research DCPSSR. All four performance evaluation metrics show that the proposed technique performs better than the current method and our previous research.

## 5. CONCLUSION

A hybrid approach for image dehazing is proposed by fusing the CAP and SSR dehazing techniques. The performance evaluation parameter such as VM is the most convincing evidence to prove the efficiency of the proposed method. Apart from PSNR and VM, MSE and SSIM are also computed. In the case of haze removal research, the significant performance evaluation parameter is VM. While considering its value for the proposed method is 134.8, whereas its only 94.3 and 108.6 in case of DCP and DCPSSR. For the proposed method, other parameters such as

PSNR, MSE and SSIM are more or less same as those of DCP and DCPSSR.This demonstrates the superiority of the proposed strategy since the value of the VM index is relatively high as compared to that of other existing methods. It is also discovered that for the proposed hybrid CAP & SSR image dehazing technique, the image dehazing has become more optimised and effective in terms of PSNR, MSE, SSIM and VM.The proposed method results in dehazed images with less distortion, lower noise levels, and improved enhancement and contrast in trials. The benefits of the proposed technique have been outlined, and several illustrated cases have been provided. When compared to standard dehazing techniques, the proposed approach has the potential to be an efficient tool for practical image haze removal. The research work may be further extended to dehaze hazy videos by using Multi Scale Retinex (MSR) method.

**REFERENCES**

1. Zhu, Q., Mai, J., & Shao, L. (2014, September). Single image dehazing using color attenuation prior. In *BMVC*
2. Balakrishnan, A., & James, S. P. (2017)Haze Removal Using Color Attenuation Prior With Varying Scattering Coefficients. *International Journal of Engineering Research and Science*, *4*(6).
3. Yu, J., Wang, Y., & Zhou, S. (2018, April). Haze removal algorithm using color attenuation prior and guided filter. In *Proceedings of the 3rd International Conference on Multimedia Systems and Signal Processing* (pp. 41-45).
4. Thepade, S. D., Mishra, P., Udgirkar, R., Singh, S., &Mengwade, P. (2018, August). Improved haze removal method using proportionate fusion of color attenuation prior and edge preserving. In *2018 Fourth International Conference on Computing Communication Control and Automation (ICCUBEA)* (pp. 1-5). IEEE.
5. Raikwar, S. C., &Tapaswi, S. (2018). An improved linear depth model for single image fog removal. *Multimedia Tools and Applications*, *77*(15), 19719-19744.
6. Huang, H., Song, J., Guo, L., Wang, H. F., & Wang, P. (2019). Haze removal method based on a variation function and color attenuation prior for UAV remote-sensing images. *Journal of Modern Optics*, *66*(12), 1282-1295.
7. Ngo, D., Lee, G. D., & Kang, B. (2019). Improved color attenuation prior for single-image haze removal. *Applied Sciences*, *9*(19), 4011.
8. Wang, Q., Zhao, L., Tang, G., Zhao, H., & Zhang, X. (2019, December). Single-image Dehazing using color attenuation prior based on haze-lines. In *2019 IEEE International Conference on Big Data (Big Data)* (pp. 5080-5087). IEEE.
9. Kansal, I., &Kasana, S. S. (2020). Improved color attenuation prior based image de-fogging technique. *Multimedia Tools and Applications*, *79*(17), 12069-12091.
10. Zhang, B., Wang, M., &Shen, X. (2021). Image haze removal algorithm based on non sub sampled contourlet transform. *IEEE Access*, *9*, 21708-21720.
11. Tang, J., Zhang, Z., Niu, L., Feng, Y., Su, B., & Lin, S. (2022, March). Research on Image Defogging Algorithms Based on Color Attenuation Prior. In *Journal of Physics: Conference Series* (Vol. 2216, No. 1, p. 012080). IOP Publishing.
12. Tang, S., Dong, M., Ma, J., Zhou, Z., & Li, C. (2017, May). Color image enhancement based on retinex theory with guided filter. In *2017 29th Chinese Control And Decision Conference (CCDC)* (pp. 5676-5680). IEEE.
13. Faraj, N. Q., &Abood, L. K. (2017). Single Scale Retinex (SSR) and Multi Scale Retinex (MSR) Enhancement Algorithms for Thermal Night-Vision Images. *Iraqi J. Sci*, 2486-2495.
14. Galdran, A., Alvarez-Gila, A., Bria, A., Vazquez-Corral, J., &Bertalmío, M. (2018). On the duality between retinex and image dehazing. In *Proceedings of the IEEE conference on computer vision and pattern recognition* (pp. 8212-8221).
15. Li, Z., Li, G., Niu, B., & Peng, F. (2018). Sea cucumber image dehazing method by fusion of retinex and dark channel. *IFAC-PapersOnLine*, *51*(17), 796-801.

16. Liu, X., Liu, C., Lan, H., &Xie, L. (2020). Dehaze enhancement algorithm based on retinex theory for aerial images combined with dark channel. *Open Access Library Journal*, *7*(4), 1-12.
17. Guo, Z., & Wang, C. (2020, November). Low Light Image Enhancement Algorithm Based on Retinex and Dehazing Model. In *2020 6th International Conference on Robotics and Artificial Intelligence* (pp. 84-90).
18. Huang, W., Zhu, Y., & Huang, R. (2020). Low light image enhancement network with attention mechanism and retinex model. *IEEE Access*, *8*, 74306-74314.
19. Saikumar, T., Srujan Raju, K., Srinivas, K., &Varaprasad Rao, M. (2018, January). Statistical Metric Measurement Approach for Hazy Images. In *International Conference on Communications and Cyber Physical Engineering 2018* (pp. 261-267). Springer, Singapore.
20. Chung, Y. L., Chung, H. Y., & Chen, Y. S. (2020). A study of single image haze removal using a novel white-patch retinex-based improved dark channel prior algorithm. *Intelligent Automation and Soft Computing*.
21. Zhuang, P., Li, C., & Wu, J. (2021). Bayesian retinex underwater image enhancement. *Engineering Applications of Artificial Intelligence*, *101*, 104171.
22. Ismail, M. K., & Al-Ameen, Z. (2022). Adapted Single Scale Retinex Algorithm for Nighttime Image Enhancement. *AL-Rafidain Journal of Computer Sciences and Mathematics*, *16*(1), 59-69.